Frequency and Voltage Control Strategy of Standalone Microgrids With High Penetration of Intermittent Renewable Generation Systems

Yun-Su Kim, *Student Member, IEEE*, Eung-Sang Kim, and Seung-Il Moon, *Senior Member, IEEE*

***Abstract*—In this paper, we propose a frequency and voltage control strategy for a standalone microgrid with high penetration of intermittent renewable generation systems, which might cause large frequency and voltage deviation in the system due to unpredictable output power fluctuations. To this end, a battery energy storage system (BESS) is suggested for generating the nominal system frequency instead of a synchronous generator, from a frequency control perspective. This makes the system frequency independent of the mechanical inertia of the synchronous generator. However, a BESS has a capacity limitation; a synchronous generator is used to maintain the state of charge (SOC) of the BESS at a certain value. For voltage control, we proposed that a reactive power/active power (Q/P) droop control be added to the conventional reactive power controller. By adding a Q/P droop control, renewable generation acquires a voltage-damping effect, which dramatically alleviates the voltage fluctuation induced by its own output power fluctuation. Simulation results prove the effectiveness of the proposed control strategy from both frequency and voltage control perspectives.**

***Index Terms*—Battery energy storage system (BESS), frequency control, Q/P droop, renewable generation, standalone microgrid, voltage control, voltage-damping effect.**

I. Introduction

STANDALONE microgrids are vulnerable to frequency and voltage deviations since they are isolated power systems that have smaller equivalent inertia and a weaker grid than a conventional power system. The high penetration of intermittent renewable generation, such as photovoltaic (PV) and wind power, makes the problem worse. With increasing environmental awareness, the penetration of renewable generation has increased gradually [1], [2]. This has led to many projects, such as [3]–[5], which attempt to interconnect renewable generation systems to isolated power systems, such as remote islands, thereby constructing a standalone microgrid. Typically, in an isolated power system, a diesel generator based on a synchronous generator generates the nominal system frequency and voltage, with the aid of active power/frequency (P/F) and reactive power/voltage (Q/V) droop control of other power generation systems and voltage-compensation devices. However, this control strategy is patterned after that of a conventional power system. A different control strategy needs to be applied to a small isolated power system, especially with the high penetration of intermittent renewable power generation, for stable frequency and voltage control.

Many studies have examined methods to support frequency control. In [6], strategies enabling wind power to operate in a manner similar to a conventional power plant were suggested for dispatching power at the operator's request. In [7], primary frequency support from deloaded wind turbines using variable droop was developed. A frequency droop control was applied to PV power generation in [8]. However, frequency control strategies using intermittent renewable generation are not beneficial economically, since they cannot maximize their ability to utilize free energy. With the introduction of the battery energy storage system (BESS), the work in [9]–[12] proposed control strategies enabling the BESS to support the system frequency. It might assist in preventing the system frequency from deviating far from its nominal value, although the deviation of the system frequency is largely dependent on the system inertia. Hence, the frequency control strategies investigated to date are not effective for isolated power systems that have small system inertia.

From a voltage-control perspective, most control strategies [13]–[17] have applied optimization algorithms to meet specific objectives, such as minimizing loss, improving the voltage profile, mitigating the voltage fluctuation, and maintaining voltage levels within regulated limits. However, these methods will never be perfectly accurate, since they are based on the forecasts of load demand, wind speed, and solar irradiance. Reference [18] suggests a voltage control strategy that considers forecast error, but still errors are inevitable. A voltage compensator can be used to improve voltage quality as proposed in [19] or to mitigate voltage fluctuation as in [17], but its installation will lead to an additional cost. The Q/V droop control is widely used for voltage compensation, but the compensation is triggered by sensing the voltage deviation. Consequently, voltage fluctuation as a result of intermittent output power is unavoidable.

In short, the research so far has attempted to resolve the frequency and voltage fluctuation problem by sensing its deviation

Manuscript received October 06, 2014; revised January 02, 2015; accepted February 23, 2015. Date of publication March 18, 2015; date of current version December 18, 2015. This work was supported by the Global Excellent Technology Innovation under Grant 20132010101890 of the Korea Institute of Energy Technology Evaluation and Planning (KETEP), granted financial resource from the Ministry of Trade, Industry & Energy, Republic of Korea. Paper no. TPWRS-01365-2014.

Y.-S. Kim and S.-I. Moon are with the School of Electrical and Computer Engineering, Seoul National University, Seoul 151-744, Korea (e-mail: yskim@powerlab.snu.ac.kr; moonsi@plaza.snu.ac.kr).

E.-S. Kim is with Korea Electrotechnology Research Institute, Changwon 642-120, Korea (e-mail: eskim@keri.re.kr).

Color versions of one or more of the figures in this paper are available online at http://ieeexplore.ieee.org.

Digital Object Identifier 10.1109/TPWRS.2015.2407392

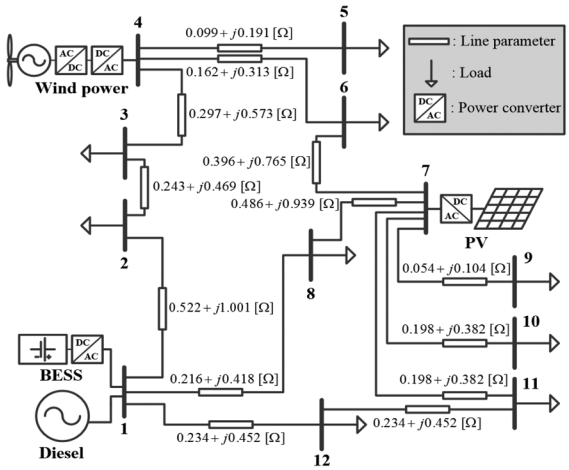

Fig. 1. Ulleungdo power system configuration.

from the nominal value. In contrast, we are focusing on the fundamental problems causing the frequency and voltage fluctuation, which are the frequency dependency on the system inertia and active output power fluctuations of the renewable generation systems. To this end, the proposed strategies include the following: 1) instead of a diesel generator, a BESS is used to generate the nominal frequency and make the system frequency independent of the mechanical inertia of a synchronous generator; 2) the diesel generator is adjusted to maintain the state of charge (SOC) of the BESS at a certain value and the reference value of the SOC is adjusted to limit the output power of the diesel generator to within an allowable range; 3) Q/P droop control, which has a damping effect on the voltage, is added to the renewable generation to prevent the voltage fluctuation induced by its own active output power fluctuations; and, above all, 4) real data including line impedances and load demand are considered to model test power system network for practical application of the proposed strategy.

The remainder of this paper is organized as follows. Section II shows the system configuration. Sections III and IV illustrate the control strategy for frequency and voltage, respectively. Section V shows the simulation results and discussion. Section VI outlines the conclusion.

II. System Configuration

The South Korean island of Ulleungdo has been designated a "green island" to make it a standalone microgrid and to realize energy self-sufficiency. Our proposed control strategy will be tested on the Ulleungdo power system presented in Fig. 1, which shows bus numbers, line parameters, loads, and power generation systems that will replace the conventional versions. The line parameters were calculated by considering the distance between loads and the location of loads were obtained from Korean Electric Power Corporation (KEPCO). The line impedance is considered as a type of ACSR 160-mm^2, 6.6-kV cable. The rates of power generation using the diesel generator, BESS, wind power, and PV power are 14, 15, 9.7, and 1 MW, respectively. The nominal system frequency and voltage are 60 Hz and 6.6 kV, respectively, and the load demands during the day and night are shown

TABLE I
System Load Demand

Bus Number	Day [MW]	Night [MW]
2	3	1.5
3	2	1
5	1	0.5
6	1	0.5
8	2	1
9	0.2	0.1
10	0.2	0.1
11	0.1	0.05
12	0.5	0.25
Total	10	5

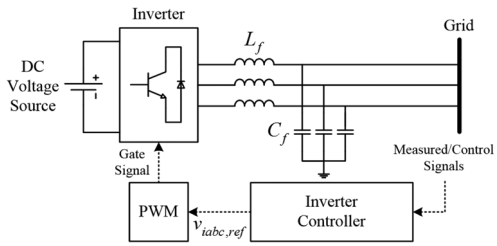

Fig. 2. Inverter-interfaced generation system.

in Table I which is based on the real data of the Ulleungdo power system referred to in [20].

The generation systems were modeled in MATLAB. Since our proposed control strategies focus mainly on the grid-side inverters, the dc-link and prime mover parts of the BESS, the PV and wind power systems are simplified as ideal dc voltage sources as shown in Fig. 2. The inverters were modeled as two-level type and sine-pulse width modulation (S-PWM) with switching frequency of 1.8 kHz was adopted to generate the gate signals of the inverter. The inverter controller provides the reference of three-phase voltage at the inverter terminal by using the control input and measured data signals. The details of controller of each generation system will be discussed in Sections III and IV.

III. Frequency Control Strategy

Since a standalone microgrid with small system inertia is vulnerable to the output power fluctuations of intermittent renewable generation systems, we propose a BESS for generation of the nominal system frequency. In a conventional isolated power system, the system frequency is formed by a synchronous generator, as shown in Fig. 3(a). Hence, the system frequency is directly related to the rotational speed of the generator rotor. With this mechanism, relationship between the electromagnetic torque and the angular velocity of the rotor is as follows [21]:

$$J\frac{d\omega_m}{dt} = T_m - T_e \tag{1}$$

where J is the combined moment of inertia of generator and turbine, ω_m is the angular velocity of the rotor, T_m is the mechanical torque, and T_e is the electromagnetic torque. From (1), it can be noticed that, if the load (T_e) is changed, the system frequency (ω_m) will be changed inversely proportional to the system inertia (J). Thus, the system frequency of an isolated

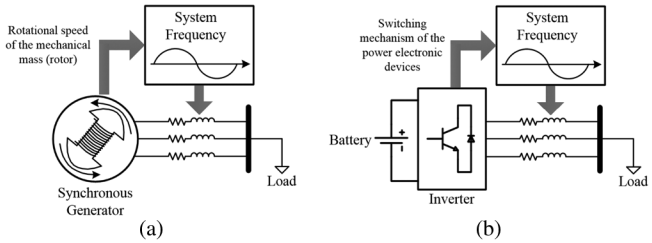

Fig. 3. Two different types of generator forming the system frequency. (a) Synchronous generator (conventional). (b) BESS (proposed).

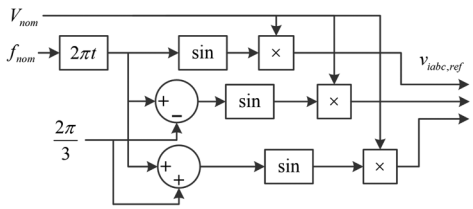

Fig. 4. Control scheme of the grid-side inverter of the BESS.

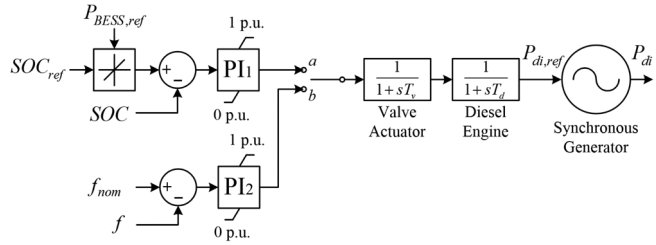

Fig. 5. Control scheme of the output active power of the diesel generator.

power system such as a standalone microgrid which has small system inertia is vulnerable to the load change. To overcome this weakness, we propose for the BESS rather than the diesel generator to form the system frequency. As shown in Fig. 3(b), the BESS forms the system frequency with the switching mechanism of the power electronic devices. Since inverters can change the output voltage angle instantaneously [22], the system frequency can be tightly held on to its nominal value by adopting the proposed method. The BESS is chosen to fulfill the proposed strategy since it has a chargeable characteristic unlike any other inverter-interfaced generation systems. This enables the BESS to take over twice amount of the load change than the others with same rate power. For instance, a 1-kW BESS is capable of taking over a 2-kW load change (from -1 to 1 kW) while the others of same rate power are capable of taking over 1-kW load change only.

To achieve the proposed strategy, the grid-side inverter of the BESS is controlled as illustrated in Fig. 4, where $V_{\rm nom}$ and $f_{\rm nom}$ are the nominal voltage and frequency, respectively, t is the simulation time, and $v_{iabc,\rm ref}$ is the reference of the three-phase inverter terminal voltage. $v_{iabc,\rm ref}$ is the input to the S-PWM, which generates gate signals for the inverter. Since the rate power of industrial BESSs keeps growing, they can now cover the load demand of small power systems. In addition, the rapid charging and discharging characteristics of the BESS can respond immediately to the output power fluctuations of renewable generation systems. However, the BESS itself can neither adjust its SOC nor implement frequency droop by using the control scheme shown in Fig. 4, since its only objective is to maintain the system frequency at the nominal value. To overcome this problem, the diesel generator is controlled as shown in Fig. 5. During normal operation, the switch shown in Fig. 5 is connected to node a and hence the diesel generator is controlled to maintain the SOC at the reference value $\rm SOC_{ref}$. This control mode acts as load-SOC control as like as load-frequency control of the conventional method. SOC is the instantaneous SOC of the BESS. In this study, $\rm SOC_{ref}$ is chosen as 0.5 p.u., arbitrarily, however it can be adjusted by an operator to charge or discharge the BESS. For instance, at heavy/light load condition, the SOC will be lower/higher than $\rm SOC_{ref}$, so, in this case, $\rm SOC_{ref}$ can be adjusted to lower/higher value. In addition, the amount of output active power of the BESS can also be controlled by adjusting the ramp rate of SOC_{ref}. This can be explained by the following equations which present the relationship between the SOC and the active power [23]:

$$\rm SOC = SOC_{\it i} - \int \frac{\it I_{\rm dc}}{\it Q} \it dt \tag{2}$$

$$I_{\rm dc} = \frac{P_{\rm BESS}}{V_{\rm dc}} \tag{3}$$

$$Q = \frac{I_{\rm dc,rate} C_{\rm BESS,rate}}{P_{\rm BESS,rate}} \tag{4}$$

where $\rm SOC_{\it i}$ is the initial value of the SOC, $I_{\rm dc}$ is the output dc current from the dc-link of the BESS, $V_{\rm dc}$ is the dc voltage of the dc-link of the BESS, $P_{\rm BESS}$ is the output active power of the BESS, $I_{\rm dc,rate}$ is the rate value of $I_{\rm dc}$, $C_{\rm BESS,rate}$ is the rate capacity of the BESS, and $P_{\rm BESS,rate}$ is the rate active power of the BESS. Substituting (3) and (4) into (2) gives

$$\rm SOC = SOC_{\it i} - \int \frac{\it P_{\rm BESS,rate} P_{\rm BESS}}{\it V_{\rm dc} I_{\rm dc,rate} C_{\rm BESS,rate}} \it dt. \tag{5}$$

Taking the derivative of (5) gives

$$\frac{d\rm SOC}{\it dt} = -\it K_r P_{\rm BESS} \tag{6}$$

where K_r is a constant value assuming that $V_{\rm dc}$ is constant. Thus, one can determine $P_{\rm BESS}$ by adjusting the ramp rate of SOC, which is $d\rm SOC/\it dt$. Consequently, the reference of the output active power of the BESS $P_{\rm BESS,ref}$ in Fig. 5 is used to adjust the ramp rate of the $\rm SOC_{ref}$. The simulation result that $P_{\rm BESS}$ is controlled by adjusting $d\rm SOC/\it dt$ will be shown in Section V. The output limiter and anti-windup function are added at the output of the proportional-integral (PI) controller to keep the output active power of the diesel generator within an allowable range, from 0 p.u. to 1 p.u. Since the system frequency is entirely depending on the BESS in this control strategy, the reliability problem may be raised due to tripping event of the BESS. To prevent this problem, the switch connection is changed from node a to b when the BESS tripped out from the system. During the switch is connected to node b, the diesel generator is controlled as same as the conventional one. The output of PI controller provides $P_{\rm di,ref}$, which is the mechanical input to the synchronous generator, via a valve actuator and a diesel engine. The synchronous generator model is referred to in the library of MATLAB/SimPowerSystems. T_v and T_d are the time constants of the valve actuator and diesel

engine, respectively and equal 0.05 and 0.5 s, respectively, as in [24]. $P_{\rm di}$ is the output active power of the diesel generator. The parameters of PI controllers and the synchronous generator are given in the Appendix.

With this control strategy, the diesel generator acts as a secondary SOC control which is a similar concept of the secondary frequency control of the conventional power system. Since the grid frequency formed by the BESS is not allowed to be changed, which means that the frequency droop control is not used, the diesel generator supports the SOC rather than the frequency. This coordinated control of the BESS and diesel generator makes the BESS operate continuously without concern for a low SOC and simultaneously makes the system frequency hold to the nominal value rigorously.

IV. Voltage Control Strategy

In this study, the system nominal voltage is maintained by the excitation system of the diesel generator. Unlike the frequency, however, the voltage problem must be resolved locally. To solve the local voltage fluctuations caused by the intermittent output power of renewable generation systems, we propose adding a Q/P droop control to the intermittent renewable generation systems, as shown in Fig. 6 where the subscript ref denotes the reference value, θ_s is the angular position of the system voltage, v_{id} and v_{iq} are the inverter terminal voltage of the d- and q-components, respectively, i_{id} and i_{iq} are the inverter terminal current of the d- and q-components, respectively, ω_s is the angular frequency of the system voltage, L_f is the filter inductance, P and Q are the output active and reactive powers, respectively, K_{QP} and K_{QV} are the Q/P and Q/V droop coefficients, respectively, P_o and Q_o are the operating points of the active and reactive power, respectively, $Q_{\rm max}$ is the maximum reactive power, and $V_{\rm bus}$ is the voltage of the bus where the renewable generation is interconnected. $P_{\rm ref}$ is the maximum power from renewable generation that can be extracted from wind speed or solar irradiance. Q_o is set to 0 so that the renewable generation systems operate as unity power factor when the voltage droop control is not activated. The parameters of PI controllers are given in the Appendix.

As a conventional control, the Q/V droop control prevents the bus voltage from deviating far from the nominal value. As in [25], K_{QV} has a value between 0 and 25 considering the rate capacity of power generation. The value of K_{QV} is based on the following equation [25]:

$$K_{QV} = \frac{\dfrac{Q}{P_{\rm rate}}}{\dfrac{\Delta V_{\rm bus}}{V_{\rm base}}} \tag{7}$$

where $V_{\rm base}$ and $P_{\rm rate}$ are the base voltage of the bus and the rate active power of the generation system, respectively. Here, K_{QV} of the PV and wind power is set to 25 and 5, respectively. Since K_{QV} is determined based on the rate capacity of power generation, adding the Q/P droop control might cause excessive reactive power output. To prevent this problem, $Q_{\rm ref}$ is limited by the following equations:

$$Q_{\rm max} = \sqrt{S_{\rm rate}^2 - P^2} \tag{8}$$

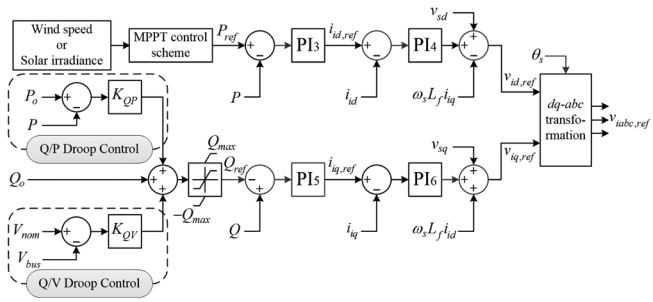

Fig. 6. Control scheme of the grid-side inverter of the renewable generation systems.

where $S_{\rm rate}$ is the rate apparent power of the inverter which is considered to be same as the rate power of generation system. From (8), it can be noticed that the maximum reactive power is determined by the output active power which means that maximizing the active power is prioritized over compensating the reactive power.

The voltage fluctuation cannot be effectively prevented by adopting the conventional Q/V droop control since it fundamentally triggered only after the voltage deviation is occurred as shown in Fig. 6. The focus of this paper is on the resolving of the fundamental problem that causes the voltage fluctuation. Thus, the role of the Q/P droop control of the renewable generation systems is to prevent voltage fluctuations induced by the system's own power fluctuations. By sensing the active power deviation from P_o, reactive power in proportion to K_{QP} is produced in compensation to prevent voltage fluctuation. This, indeed, has a damping effect on the voltage fluctuation caused by active output power fluctuation as will be shown later in Section V.

Day and night are considered separately to determine P_o and K_{QP}. P_o for the PV and wind power is calculated by applying the average value of solar irradiance and wind speed, respectively. K_{QP} is obtained using a sensitivity matrix, which can be calculated from the Jacobian matrix equation given in [26]

$$\begin{bmatrix} \Delta \boldsymbol{P} \\ \Delta \boldsymbol{Q} \end{bmatrix} = \begin{bmatrix} \boldsymbol{J_{P\theta}} & \boldsymbol{J_{P|V|}} \\ \boldsymbol{J_{Q\theta}} & \boldsymbol{J_{Q|V|}} \end{bmatrix} \begin{bmatrix} \Delta \boldsymbol{\theta} \\ \Delta |\boldsymbol{V}| \end{bmatrix} \tag{9}$$

where $\Delta \boldsymbol{P} = [\Delta P_1, \Delta P_2, \ldots, \Delta P_{12}]^{\rm T}$ is the active power deviation at each bus, $\Delta \boldsymbol{Q} = [\Delta Q_1, \Delta Q_2, \ldots, \Delta Q_{12}]^{\rm T}$ is the reactive power deviation at each bus, $\Delta \boldsymbol{\theta} = [\Delta \theta_1, \Delta \theta_2, \ldots, \Delta \theta_{12}]^{\rm T}$ is the voltage angular position deviation at each bus, $\Delta |\boldsymbol{V}| = [\Delta |V|_1, \Delta |V|_2, \ldots, \Delta |V|_{12}]^{\rm T}$ is the voltage magnitude deviation at each bus, and $\boldsymbol{J_{P\theta}}$, $\boldsymbol{J_{Q\theta}}$, $\boldsymbol{J_{P|V|}}$, and $\boldsymbol{J_{Q|V|}}$ are the Jacobian matrices. Note that the Jacobian matrix can become ill-conditioned or singular if the network voltage level is low. In this case, another method should be developed for acquiring Q/P droop coefficient. However, we focus on the medium or higher level of distribution network in this study. Taking the inverse transform of the Jacobian matrix given in (9), the sensitivity matrix equation can be expressed as

$$\begin{bmatrix} \Delta \boldsymbol{\theta} \\ \Delta |\boldsymbol{V}| \end{bmatrix} = \begin{bmatrix} \boldsymbol{S_{\theta P}} & \boldsymbol{S_{\theta Q}} \\ \boldsymbol{S_{|V|P}} & \boldsymbol{S_{|V|Q}} \end{bmatrix} \begin{bmatrix} \Delta \boldsymbol{P} \\ \Delta \boldsymbol{Q} \end{bmatrix}. \tag{10}$$

The voltage deviation occurring with the change in the active and reactive power is calculated as

$$\Delta|\boldsymbol{V}| = \boldsymbol{S}_{|\boldsymbol{V}|\boldsymbol{P}}\Delta\boldsymbol{P} + \boldsymbol{S}_{|\boldsymbol{V}|\boldsymbol{Q}}\Delta\boldsymbol{Q}. \quad (11)$$

From (11), it can be noticed that the voltage fluctuation can be occurred by the active power fluctuation and can be reduced by compensation of the reactive power. The objective of the Q/P droop control is to mitigate the bus voltage fluctuation caused by the output power fluctuation of the renewable generation systems that are interconnected to that bus. Hence, to make the voltage deviation of bus i equal 0, the following equation must be satisfied:

$$\begin{aligned}\Delta|V|_i &= S_{|V|P,i,i}\Delta P_i + S_{|V|Q,i,i}\Delta Q_i \\ &= 0 \\ &= S_{|V|P,i,i}(P_{o,i} - P_i) + S_{|V|Q,i,i}(Q_{o,i} - Q_i). \quad (12)\end{aligned}$$

Since $Q_{o,i}$ is set to 0, (12) can be rearranged as

$$Q_i = \left(\frac{S_{|V|P,i,i}}{S_{|V|Q,i,i}}\right)(P_{o,i} - P_i) \quad (13)$$

where $S_{|V|P,i,i}/S_{|V|,Q,i,i}$ is determined to be K_{QP} of the renewable generation interconnected at bus i. Determining proper P_o is in the scope of the system scheduling, so it will not be discussed in this paper.

V. Simulation Results and Discussion

To prove the effectiveness of the proposed control method, three control methods-without the P/F and Q/V droop control method, with the P/F and Q/V droop control method, and with the proposed control method-are compared with each other during the day and at night. The P/F droop coefficient of the BESS used in this study is 10. Since the simulation time scale is roughly tens of seconds, the capacity of the BESS is scaled down to 1/20 of its practical value, 30 MWh, in the simulation to illustrate the change in the SOC clearly. To account for realistic situation, in Cases I and II, the data of wind speed and solar irradiance are considered to be similar to real data referred to in [27], [28]. Case III accounts for the worst case where wind speed and solar irradiance are change from the minimum to the rate value. The load change and the tripping of the BESS are considered in Case IV. In Case V, only the variation of the solar irradiance (assuming that the wind speed is constant) is considered to ensure the proposed method performs well for the PV power system bus. Finally, the charging/discharging ability of the BESS by controlling the ramp rate of the SOC is tested in Case VI. The simulation was modeled and implemented with MATLAB/SimPowerSystems.

A. Case I—Day Time

In the day time, the wind speed ranges from 10.5 to 11.5 m/s and averages 11 m/s [27], [28]. The solar irradiance ranges from 600–720 W/m^2 and averages 660 W/m^2 [27], [28]. The load demand is shown in Table I. Based on day-time data, the K_{QP} of the wind and PV power are calculated to be 0.413 and 0.495, respectively.

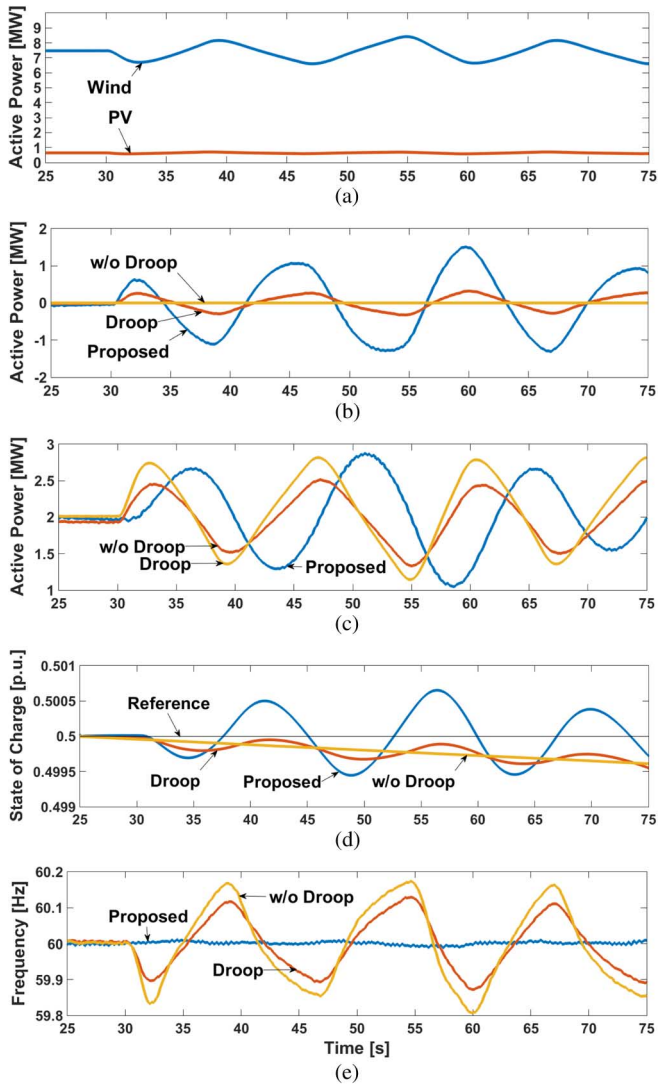

Fig. 7. Frequency control results for Case I. (a) Active power of wind and PV. (b) Active power of BESS. (c) Active power of diesel generator. (d) SOC. (e) Frequency.

Fig. 7(a) shows the output active power of the PV and wind power and Fig. 7(b) and (c) show the output active power of the BESS and diesel generator, respectively, for the three different control methods. Without droop control, the diesel generator takes full responsibility for the output fluctuations of the renewable generation systems, while the BESS does nothing. With the droop control, the BESS supports the diesel generator with P/F droop control, although the diesel generator still strives to match the power demand. Conversely, the roles of the two power generation systems are exchanged with our proposed control method. The BESS responds immediately to any output power fluctuations, whereas the diesel generator is used to maintain the SOC, thereby supporting the BESS. Fig. 7(d) shows the SOC of the three control methods and the reference SOC for the proposed control method. There are the oscillations of the SOC around at the desired level in the proposed method. This is due to the slow dynamics of the diesel generator and

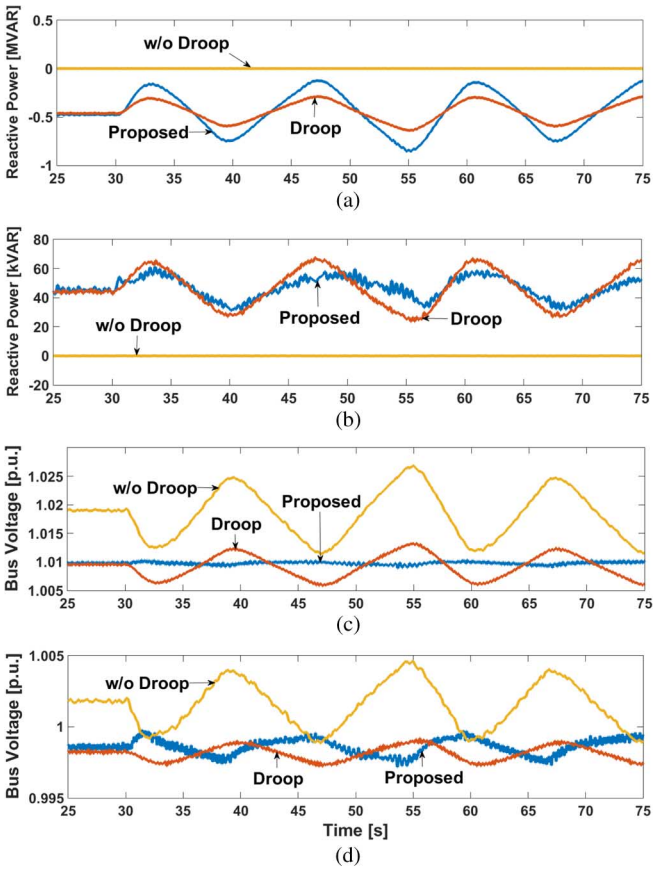

Fig. 8. Voltage control results for Case I. (a) Reactive power of wind power. (b) Reactive power of PV power. (c) Bus voltage of wind power. (d) Bus voltage of PV power.

the fluctuations of active powers of renewable generation systems. However, the SOC can be stabilized to the desired level if there are no fluctuations of the active powers as it will be shown in Case IV. Without droop control, although the active output power of the BESS is close to 0 MW, the SOC decreases slightly due to small losses, such as the filter and inverter switching losses. Using the droop control method, the SOC fluctuates as the BESS supports the diesel generator, although its trend line is similar to that without the droop control. Nevertheless, although it fluctuates, the SOC is maintained at the reference value. As shown in Fig. 7(e), the frequency deviates from its nominal value without droop control. With droop control, the deviation is mitigated, but is still not prevented completely. With these two methods, the deviation and restoration of the frequency are dependent on the rotational speed and inertia of the synchronous generator. In comparison, with the proposed control method, the system frequency is generated by the BESS, which has rapid response characteristics and no mechanically rotating mass. Consequently, the frequency rarely deviates from its nominal value.

Fig. 8(a) and (b) show the reactive power of the wind and PV power, respectively. Without droop control, both renewable generation systems have the same power factor, whereas applying the Q/V droop control, they control the reactive power to compensate for the voltage deviation. Applying the proposed control method, the reactive powers of both renewable generation systems are controlled not only for compensating for voltage deviation but also for mitigating the voltage fluctuation induced by their own active power fluctuations. In the case of PV power, there is little difference between the conventional droop control method and the proposed control method, since the output active power fluctuation is not very large. By contrast, in the case of wind power, the proposed control method outputs more reactive power than the droop control method due to its large active power fluctuations. Fig. 8(c) and (d) show the bus voltages of the wind and PV power, respectively. This shows that by using the Q/V droop control, the bus voltage can be kept closer to the nominal value than without the droop control. However, it cannot effectively prevent the voltage fluctuations incurred by the output power fluctuations. By adding Q/P droop control, the voltage fluctuation can be eliminated. While the mitigation of the PV power bus voltage fluctuation is negligible, since its active power fluctuation is not very large, the wind power bus voltage fluctuation is reduced dramatically. Therefore, the proposed Q/P droop control of the renewable generation systems has a damping effect on the voltage fluctuation incurred by its own active power fluctuation.

B. Case II—Night Time

At night, the wind speed ranges from 7.1–10.2 m/s and averages 8.5 m/s [27], [28]. A solar irradiance is 0 $\mathrm{W/m^2}$ and the load demand is as shown in Table I. Based on night-time data, the calculated K_{QP} of the wind and PV power is 0.473 and 0.514, respectively.

Fig. 9(a) shows the output active power of the PV and wind power and Fig. 9(b) and (c) show the output active power of the BESS and diesel generator, respectively. At the beginning of the simulation, the BESS is set to charge 2 MW, since the total generation exceeds the load demand. The output power responses are similar to those during the day, while the output power of the diesel generator tends to fall below its minimum at 38 s and 66 s in the simulation. At these times, the $\mathrm{SOC_{ref}}$ is increased, as shown in Fig. 9(d), to increase the diesel generator active power. Consequently, the active power of the diesel generator can be operated within the allowable range. As Fig. 9(e) shows, the frequency deviation becomes greater than that during the day when applying the conventional methods, whereas the proposed method maintains the frequency at the nominal value.

The voltage control results are shown in Fig. 10. Since the output power fluctuation of the wind power is greater than that during the day, more reactive power is compensated for than during the day using the proposed control method. By contrast, for the PV power, there is little difference between the droop and proposed control methods, since the solar irradiance at night is 0 $\mathrm{W/m^2}$. Voltage fluctuation is prevented, as shown in Fig. 10(c) despite the marked wind speed fluctuation. The bus voltage of the PV power differs little between the droop and proposed control methods since there is no solar irradiance.

C. Case III—Worst Case

This case study deals with the worst case where wind speed and solar irradiance vary from 0 to the rate value. Since the solar irradiance has to be considered, the load demand is same as the day time. Hence, based on day-time data, the K_{QP} of the wind and PV power are calculated to be 0.413 and 0.495, respectively.

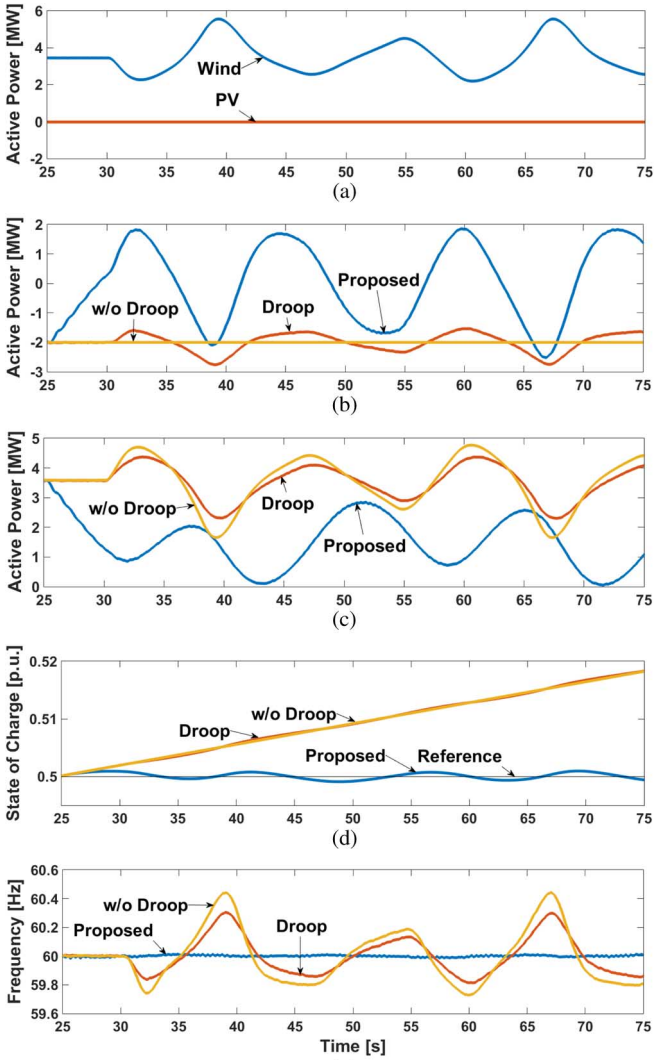

Fig. 9. Frequency control results for Case II. (a) Active power of wind and PV. (b) Active power of BESS. (c) Active power of diesel generator. (d) SOC. (e) Frequency.

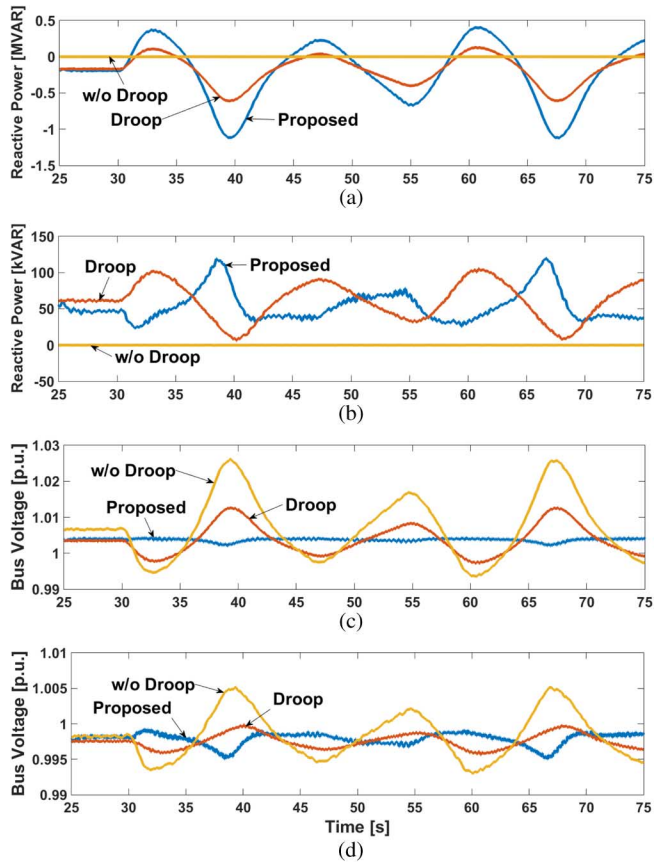

Fig. 10. Voltage control results for Case II. (a) Reactive power of wind power. (b) Reactive power of PV power. (c) Bus voltage of wind power. (d) Bus voltage of PV power.

As shown in Fig. 11(a), the active powers of wind and PV power generation systems vary from 0 to the rated value. Fig. 11(b)–(e) show the simulation results for frequency control. Due to severer fluctuations of wind speed and solar irradiance than those of Cases I and II, the SOC fluctuates more than those of Cases I and II for the proposed method. However, the frequency is tightly maintained at the nominal value still. Fig. 12 presents the simulation results for voltage control. In the proposed method, there are several points where the reactive powers of PV and wind power are limited according to (8). They are occurred at around 41, 56, and 68 s of the simulation time as shown in Fig. 12(a) and (b). As a result that can be shown in Fig. 12(c) and (d), there are little bounces of voltage around those points, but still the proposed method performs better than the others.

D. Case IV—Load Change and Tripping of the BESS

Two cases considering the proposed frequency control strategy are shown in this case study. One of them accounts for load change and the other accounts for tripping of the BESS.

Fig. 13 shows the results for the load change in the day time while the renewable generation systems output constant active power. About 0.5 MW of step load decrement is occurred at 30 s of the simulation time. Compared to Cases I, II, and III, the SOC is well converged to the reference value as shown in Fig. 13(b) since there are no other disturbances. The frequency is also well maintained to the nominal value as shown in Fig. 13(c).

The simulation results for the case of tripping of the BESS are shown in Fig. 14. If the BESS is tripped out from the system at 30 s of the simulation time as shown in Fig. 14(a) due to cases such as a fault, a maintenance, and etc., the diesel generator changes its operation mode by changing its switch (shown in Fig. 5) from node a to b. This makes the diesel generator to operate as same as the conventional one. Consequently, the frequency behaves as same as the conventional method as shown in Fig. 14(b).

E. Case V—Considering PV Bus Only

Through Cases I to III, the proposed voltage control strategy performs well for the wind power system bus whereas it barely affects the PV power system bus. A major reason for this is because that the active power fluctuation of wind power system is much larger than PV power system. So in this case, we consider the active power fluctuation of the PV power system only while the wind power system outputs constant power to make sure that

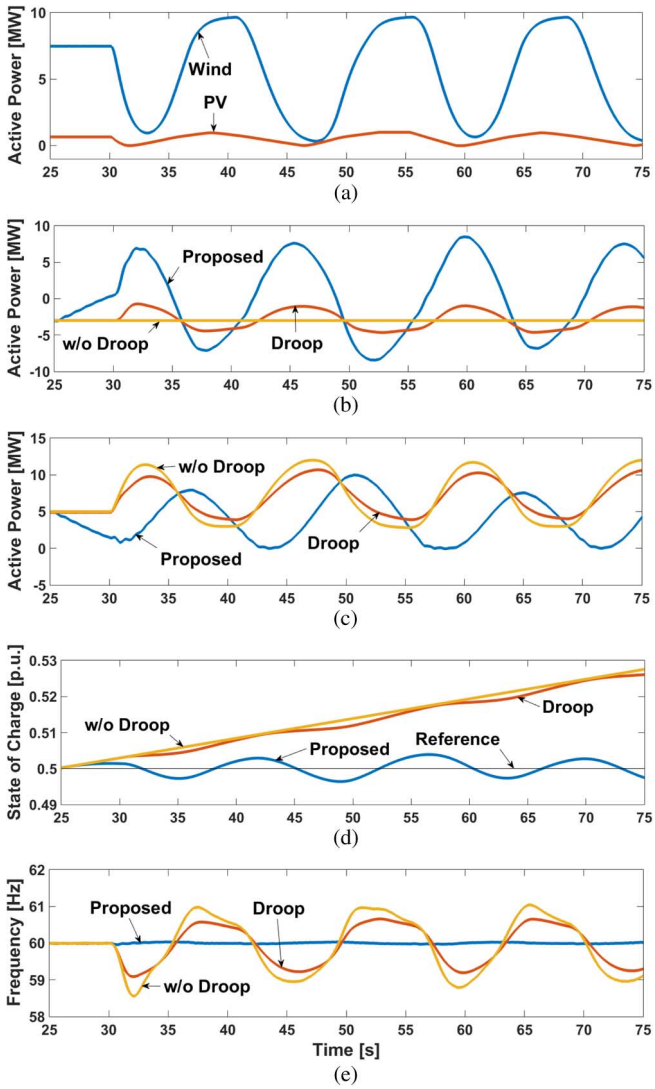

Fig. 11. Frequency control results for Case III. (a) Active power of wind and PV. (b) Active power of BESS. (c) Active power of diesel generator. (d) SOC. (e) Frequency.

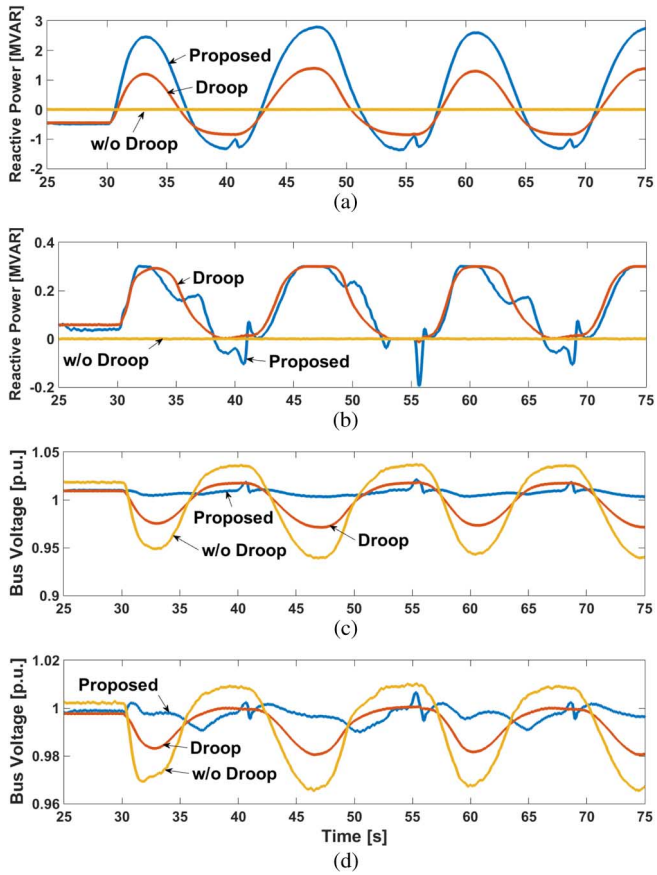

Fig. 12. Voltage control results for Case III. (a) Reactive power of wind power. (b) Reactive power of PV power. (c) Bus voltage of wind power. (d) Bus voltage of PV power.

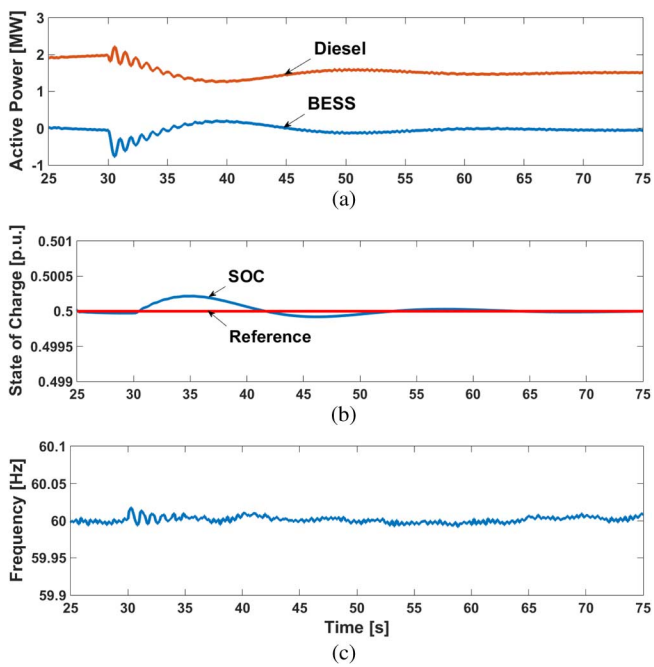

Fig. 13. Load change simulation results for Case IV. (a) Active power of BESS and diesel generator. (b) SOC. (c) Frequency.

the proposed voltage control strategy also positively affects the PV power system bus.

As shown in Fig. 15, the proposed method performs well for the PV power system also. However, if the reactive power is limited according to (8) as shown in Fig. 15(a) at around 53–56 s, the bus voltage became to have as similar value as that of the method adopting Q/V droop only.

F. Case VI—Adjusting Charge/Discharge of the BESS

The proposed strategies indeed have many advantages in the perspective of mitigating the frequency and voltage fluctuations and maintaining the SOC at the desired value. However, in the energy efficiency perspective, the BESS should be controllable. Therefore, this case study shows the availability of the BESS to be controlled at the desired level of power.

By adjusting the ramp rate of SOC shown in (6), the BESS can be controlled to output the desired level of active power. In Fig. 16(a), the ramp rate of the SOC is adjusted for the BESS to charge 1 MW. As a result that can be shown in Fig. 16(b), the diesel generator increments its output power and the BESS outputs −1 MW of active power. Similarly, the ramp rate of the

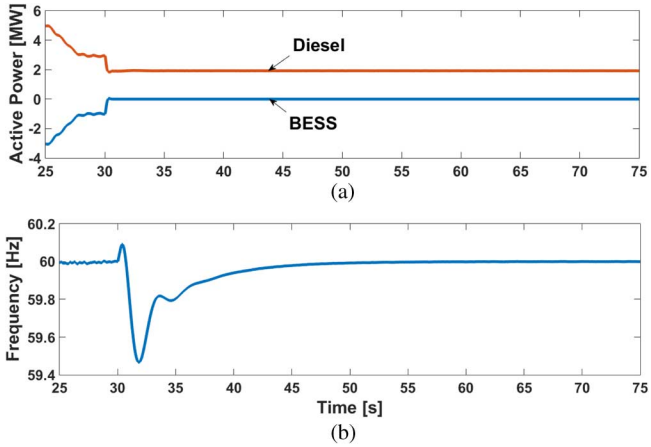

Fig. 14. BESS tripping simulation results for Case IV. (a) Active power of BESS and diesel generator. (b) Frequency.

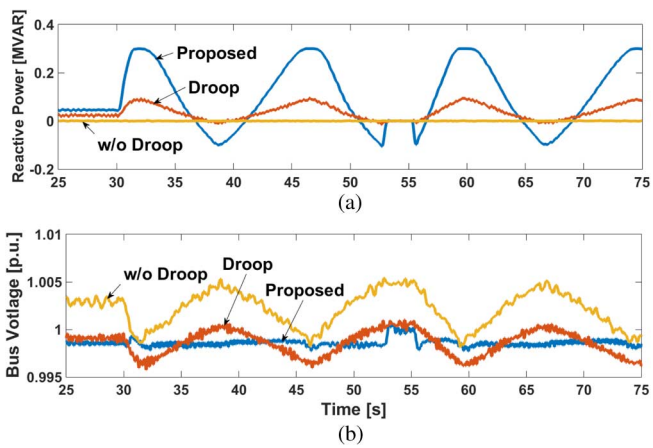

Fig. 15. Simulation results for Case V. (a) Reactive power of PV power. (b) Bus voltage of PV power.

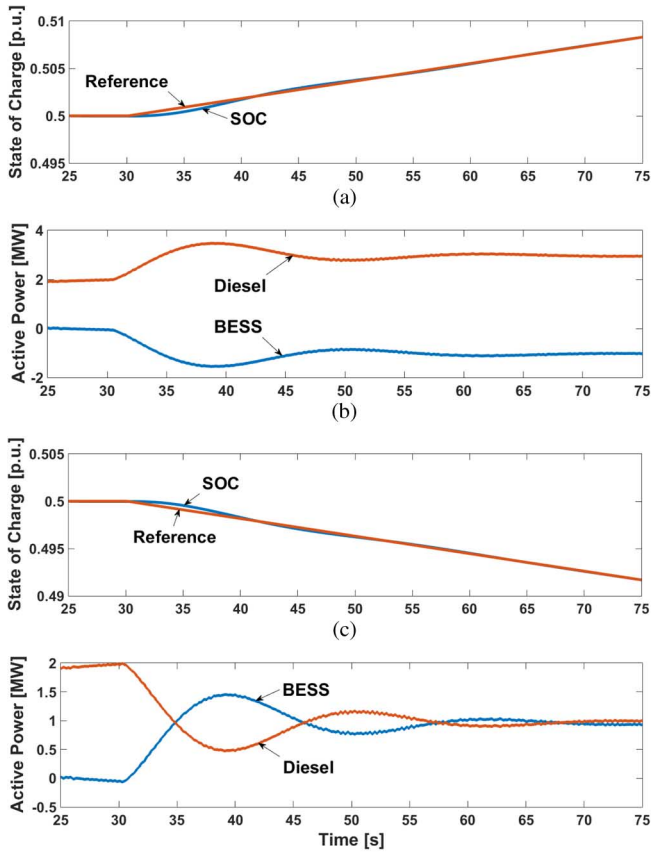

Fig. 16. Simulation results for Case VI. (a) Active power of BESS and diesel generator during charging. (b) SOC during charging. (c) Active power of BESS and diesel generator during discharging. (d) SOC during discharging.

BESS is adjusted to discharge the BESS as shown in Fig. 16(c). Consequently, the diesel generator decrements its output and the BESS outputs 1 MW of active power. In this way, the BESS can be controlled to output any desired amount of active power indirectly by adjusting the SOC ramp rate controller which is included in the controller of diesel generator.

G. Discussion

By adopting the proposed control strategies, the frequency and voltage fluctuation is drastically reduced. With this control strategy, intermittent renewable generation systems such as wind and solar power can be highly penetrated to an isolated power system regardless of the size of system inertia and strength of grid network. It has many advantages in the perspective of mitigating the frequency and voltage fluctuations, maintaining the SOC at the desired level, and the energy efficiency. Consequently, the proposed method can give us a solution to the future grid since it enables reduction of greenhouse gas by integrating large scale renewable generation systems and also enables stable operation of isolated power systems.

However, sensing the SOC of the BESS might cause another problem. For instance, in a conventional power grid, the load sharing is based on the frequency which is globally same variable and hence it can be measured from any points of the system. In contrast, the load change cannot be sensed by the frequency since it barely changed in the proposed strategy. Instead, the SOC is used to sense the load change, which means that communication infrastructure is necessary to send the SOC data to other generators for load sharing. Besides, small-signal stability is not yet analyzed and a Q/P droop coefficient might not be acquired for a low voltage distribution network. Consequently, new load sharing method for the system of multi-generators, small-signal stability analysis, and a method for acquiring Q/P droop coefficient for low voltage distribution network should be investigated for the future works.

VI. Conclusion

This paper presents a strategy for controlling the frequency and voltage of a standalone microgrid, which has low system inertia and a weak grid, with high penetration of intermittent renewable generation systems. The proposed control strategy is designed for the problem resulting from the unpredictable output active power of renewable generation systems. For stable frequency control, a BESS is used to generate the nominal system frequency, instead of the synchronous generators. This makes the system frequency independent of the mechanical inertia. In addition, the rapid response of the BESS results

TABLE II
PARAMETERS OF SYNCHRONOUS GENERATOR

Parameter	Value	Unit
X_d	1.305	p.u.
X'_d	0.296	p.u.
X''_d	0.252	p.u.
X_q	0.474	p.u.
X''_q	0.243	p.u.
X_l	0.18	p.u.
R_s	0.003	p.u.
T'_{do}	4.49	s
T''_{do}	0.0681	s
T''_q	0.0513	s
H	3.7	s

TABLE III
PARAMETERS OF PI CONTROLLERS

Controller	Kp	Ki
PI_1	80	30
PI_2	20	4
PI_3	0.4	40
PI_4	50	100
PI_5	0.4	40
PI_6	50	100

in stable operation of the frequency without deviation. The diesel generator is used to maintain the SOC of the BESS; moreover, it is controlled so as not to exceed its operational boundaries by adjusting the reference of the SOC. For stable voltage control, the Q/P droop control is added to the reactive power controller of the renewable generation systems. The Q/P droop coefficient is calculated using the sensitivity matrix. With this control, the voltage fluctuation induced by the output active power fluctuation is effectively prevented as if there is a voltage-damping effect in the renewable generation. The proposed control strategy was verified by applying it to the Ulleungdo power system, which was modeled and simulated using MATLAB/SimPowerSystems. With the proposed control strategy, increased penetration of intermittent renewable generation systems in isolated power systems is anticipated.

APPENDIX

Tables II and III show the parameters of the synchronous generator and the PI controllers, respectively.

REFERENCES

[1] Int. Energy Agency, "Photovoltaic Power Systems Programme, trends in photovoltaic applications-Survey report of selected IEA countries between 1992 and 2012," IEA-PVPS T1-23:2013, 2013.

[2] R. Thresher, M. Robinson, and P. Veers, "To capture the wind," *IEEE Power Energy Mag.*, vol. 5, no. 6, pp. 34–46, Nov./Dec. 2007.

[3] Ministry of Trade, Industry and Energy, Seoul, Korea, "2014 Business Planning Report," Feb. 2014 [Online]. Available: http://www.motie.go.kr/motie/mi/tn/planreport/presidentbriefing/bbs/bbsView.do?bbs_seq_n=12&bbs_cd_n=38

[4] M. Saastamoinen, "Case Study 18: Samsø—Renewable Energy Island Programme," NCRC, Samsø Island, Denmark, Mar. 2009 [Online]. Available: http://www.energychange.info/casestudies/175-samso-renewa ble-energy-island

[5] S. Ottewell, "Ireland's renewable island," *IET Power Eng.*, vol. 17, no. 3, pp. 10–11, Jun./Jul. 2003.

[6] L.-R. Chang-Chien and Y.-C. Yin, "Strategies for operating wind power in similar manner of conventional power plant," *IEEE Trans. Energy Convers.*, vol. 24, no. 4, pp. 926–934, Dec. 2009.

[7] K. V. Vidyanandan and N. Senroy, "Primary frequency regulation by deloaded wind turbines using variable droop," *IEEE Trans. Power Syst.*, vol. 28, no. 2, pp. 837–846, May 2013.

[8] H. Xin *et al.*, "A new frequency regulation strategy for photovoltaic systems without energy storage," *IEEE Trans. Sustain. Energy*, vol. 4, no. 4, pp. 985–993, Oct. 2013.

[9] G. Delille, B. François, and G. Malarange, "Dynamic frequency control support by energy storage to reduce the impact of wind and solar generation on isolated power system's inertia," *IEEE Trans. Sustain. Energy*, vol. 3, no. 4, pp. 931–939, Oct. 2012.

[10] I. Serban and C. Marinescu, "Control strategy of three-phase battery energy storage systems for frequency support in microgrids and with uninterrupted supply of local loads," *IEEE Trans. Power Electron.*, vol. 29, no. 9, pp. 5010–5020, Sep. 2014.

[11] I. Serban, R. Teodorescu, and C. Marinescu, "Energy storage systems impact on the short-term frequency stability of distributed autonomous microgrids, an analysis using aggregate models," *IET Renew. Power Gener.*, vol. 7, no. 5, pp. 531–539, 2013.

[12] J.-Y. Kim *et al.*, "Cooperative control strategy of energy storage system and microsources for stabilizing the microgrid during islanded operation," *IEEE Trans. Power Electron.*, vol. 25, no. 12, pp. 3037–3048, Dec. 2010.

[13] V. Calderaro *et al.*, "Optimal decentralized voltage control for distribution systems with inverter-based distributed generators," *IEEE Trans. Power Syst.*, vol. 29, no. 1, pp. 230–241, Jan. 2014.

[14] L. F. Ochoa and G. P. Harrison, "Minimizing energy losses: Optimal accommodation and smart operation of renewable distributed generations," *IEEE Trans. Power Syst.*, vol. 26, no. 1, pp. 198–205, Feb. 2011.

[15] M. Falahi, K. Butler-Purry, and M. Ehsani, "Dynamic reactive power control of islanded microgrids," *IEEE Trans. Power Syst.*, vol. 28, no. 4, pp. 3649–3657, Nov. 2013.

[16] Y.-J. Kim, "Optimal control of DG output voltage considering switching operation of ULTC and SC in distribution power systems" M.S. thesis, Dept. Elect. and Comput. Eng., Seoul Nat. Univ., Seoul, Korea, Aug. 2010 [Online]. Available: http://library.snu.ac.kr/search/DetailVie w.ax?sid=1&cid=3441592

[17] A. Elnady and Y.-F. Liu, "A practical solution for the current and voltage fluctuation in power systems," *IEEE Trans. Power Del.*, vol. 27, no. 3, pp. 1339–1349, Jul. 2012.

[18] Z. Ziadi *et al.*, "Optimal voltage control using inverters interfaced with PV systems considering forecast error in a distribution system," *IEEE Trans. Sustain. Energy*, vol. 5, no. 2, pp. 682–690, Apr. 2014.

[19] T.-L. Lee, S.-H. Hu, and Y.-H. Chan, "D-STATCOM with positive-sequence admittance and negative-sequence conductance to mitigate voltage fluctuations in high-level penetration of distributed-generation systems," *IEEE Trans. Ind. Electron.*, vol. 60, no. 4, pp. 1417–1428, Apr. 2013.

[20] Ministry of Knowledge Economy, Seoul, Korea, "The 6th Basic Plan for Long-term Electricity Supply and Demand (2013–2027)," Feb. 2013 [Online]. Available: http://www.kpx.or.kr/KOREAN/servlet/PDController?cmd=view&cd_cate=&cd_code=pds&menu_idx=108&idx=758&curpage=0&lst_type=0&lst_word=±????1

[21] P. Kundur, *Power System Stability and Control*. New York, NY, USA: McGraw-Hill, 1994.

[22] R. Majumder, A. Ghosh, G. Ledwich, and F. Zare, "Power management and power flow control with back-to-back converters in a utility connected microgrid," *IEEE Trans. Power Syst.*, vol. 25, no. 2, pp. 821–834, May 2010.

[23] L. Gao, S. Liu, and R. A. Dougal, "Dynamic lithium-ion battery model for system simulation," *IEEE Trans. Compon. Packag. Technol.*, vol. 25, no. 3, pp. 495–505, Sep. 2002.

[24] S. A. Papathanassiou and M. P. Papadopoulos, "Dynamic characteristic of autonomous wind-diesel systems," *Renewable Energy*, vol. 23, no. 2, pp. 293–311, Jun. 2001.

[25] J. MacDowell, "Installations connected to a power transmission system and generating equipment: Minimum design requirements, equipment, operations, commissioning and safety," NERC Corp., Atlanta, GA, USA, Nov. 2009 [Online]. Available: http://www.nerc.com/comm/PC/Integration%20of%20Variable%20Generation%20Task%20Force%20IVGT/Sub%20Teams/Interconnection/Spanish%20Grid%20Code_En_Translation.pdf

[26] A. R. Bergen and V. Vittal, *Power Systems Analysis*, 2nd ed. Upper Saddle River, NJ, USA: Prentice-Hall, 2006.

[27] H.-Y. Jung *et al.*, "A study on the operating characteristics of SMES for the dispersed power generation system," *IEEE Trans. Appl. Supercond.*, vol. 19, no. 3, pp. 2028–2031, Jun. 2009.
[28] A.-R. Kim *et al.*, "Performance analysis of a toroid-type HTS SMES adopted for frequency stabilization," *IEEE Trans. Appl. Supercond.*, vol. 21, no. 3, pp. 1367–1370, Jun. 2011.

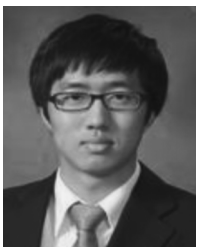

Yun-Su Kim (S'14) received the B.S. degree in electrical engineering from Seoul National University, Seoul, Korea, in 2010, where he is currently working toward the Ph.D. degree in electrical engineering.

His research interests include distributed generation, renewable energy resources, and microgrid.

Eung-Sang Kim received the M.S. and Ph.D. degreed in electric engineering from Soong-Sil University, Seoul, Korea, in 1991 and 1997, respectively. His dissertation was titled "A study on the interconnection of battery energy storage system to power distribution systems."

He has been a Team Leader in the Smart Distribution Research Center, Korea Electrotechnology Research Institute (KERI), Changwon, Korea, since 1991. His research interests are in the areas of power quality, dispersed generating system integration and application, and grid-connection of dispersed generations. He had many patents and research experiences about microgrid, renewable energy system and energy storage system.

Seung-Il Moon (M'93–SM'14) received the B.S. degree in electrical engineering from Seoul National University, Seoul, Korea, in 1985, and the M.S. and Ph.D. degrees in electrical engineering from The Ohio State University, Columbus, OH, USA, in 1989 and 1993, respectively.

Currently, he is a Professor with the School of Electrical Engineering and Computer Science, Seoul National University, Seoul, Korea. He is the Editor-in-Chief of the *Journal of Electrical Engineering and Technology*. His special fields of interest include power quality, flexible ac transmission systems, renewable energy, and distributed generation.